

# Extracellular Acidification Elicits Spatially and Temporally Distinct $\text{Ca}^{2+}$ Signals

Wan-Chen Huang,<sup>1</sup> Pawel Swietach,<sup>2</sup>  
Richard D. Vaughan-Jones,<sup>2</sup> Olaf Ansorge,<sup>3</sup>  
and Maike D. Glitsch<sup>1,\*</sup>

<sup>1</sup>Department of Physiology, Anatomy, and Genetics

<sup>2</sup>Proton Transport Group

Sherrington Building

Oxford University

Parks Road

Oxford OX1 3PT

United Kingdom

<sup>3</sup>Department of Neuropathology

John Radcliffe Hospital

Headley Way

Headington, Oxford OX3 9DU

United Kingdom

## Summary

Extracellular acidification accompanies neoplastic transformation of tissues and increases with tumor aggressiveness [1, 2]. The intracellular signaling cascade triggered by this process remains poorly understood and may be linked to recently discovered proton-activated G protein-coupled receptors such as OGR1 and G2A [3, 4]. Here, we report that OGR1 and G2A are expressed in human medulloblastoma tissue and its corresponding neuronal cell line. We show that extracellular acidification activates phospholipase C,  $\text{IP}_3$  formation, and subsequent  $\text{Ca}^{2+}$  release from thapsigargin-sensitive stores in neurons. The number of responsive cells and the amount of  $\text{Ca}^{2+}$  released from stores correlated positively with the extent of extracellular acidification.  $\text{Ca}^{2+}$  release recruited the MEK/ERK pathway, providing a mechanistic explanation for how acidification stimulates cell growth. In addition, acidification activated  $\text{Ca}^{2+}$ -permeable ion channels through a mechanism dependent on phospholipase C but independent of store depletion or a cytoplasmic  $\text{Ca}^{2+}$  rise. Hence, extracellular acidification, to levels seen in tumor tissue, activates temporally and spatially distinct pathways that elevate  $\text{Ca}^{2+}$  and may be directly relevant for tumor cell biology.

## Results and Discussion

A novel class of G protein-coupled receptor (including OGR1 and G2A) has been discovered that responds to extracellular acidification by releasing  $\text{Ca}^{2+}$  from intracellular stores [3, 4]. Reverse transcriptase-polymerase chain reaction (RT-PCR) experiments from a human cerebellar granule cell tumor (medulloblastoma) cell line (DAOY) with primers specific for OGR1 and G2A revealed the presence of both of these receptors (Figure 1A; it should be noted that a role for G2A as proton sensor is under debate [4]). Moreover, by using nine distinct samples of primary human medulloblastoma tissue, we found that all samples showed high levels of expression of the

receptors (Figure 1A and data not shown). Hence, OGR1 and G2A expression is found in both cultured cerebellar tumor cells and native cerebellar tumor tissue.

These receptors are functionally active because extracellular acidification to pH 6, a level commonly seen in tumors [5], evoked a  $\text{Ca}^{2+}$  signal when cells were bathed in  $\text{Ca}^{2+}$ -free solution, indicating  $\text{Ca}^{2+}$  release from intracellular stores (Figure 1B). We were interested to see how extracellular acidification led to  $\text{Ca}^{2+}$  release. Evidence that this included activation of phospholipase C was provided from experiments in which DAOY cells were exposed to the phospholipase C inhibitor U73122 (Figure 1C, solid line). In the presence of U73122, extracellular acidification did not trigger  $\text{Ca}^{2+}$  release from stores. Exposure of cells to the inactive U73122 analog U73343 had no effect at all (Figure 1C, dotted line). Extracellular acidification gave rise to a rapid increase in  $\text{IP}_3$  levels (Figure 2E), demonstrating that the pH-sensing receptor couples to  $\text{Ca}^{2+}$  release from intracellular stores via phospholipase C activation and subsequent  $\text{IP}_3$  production. To confirm this, we preincubated cells with the  $\text{IP}_3$  receptor blocker 2-APB (between 60 and 80 min incubation time) and found that the increase in intracellular  $\text{Ca}^{2+}$  concentration was significantly reduced in the presence of 2-APB ( $p < 0.0001$ , unpaired Student's *t* test; Figure 1D). We also preincubated cells with the sarcoplasmic and endoplasmic reticulum calcium ATPase (SERCA) pump blocker thapsigargin, which depletes intracellular  $\text{IP}_3$ -sensitive  $\text{Ca}^{2+}$  stores. Extracellular acidification now failed to induce  $\text{Ca}^{2+}$  release from stores in 18 out of 22 cells (Figure 1E). In the four responding cells, the pH-induced  $\text{Ca}^{2+}$  response was significantly smaller than that observed in control cells (Figure 1F). Preincubation of cells with ryanodine failed to affect the response to extracellular acidification (Figures 1E and 1F).

To determine the extracellular pH range over which the receptor was activated, we varied external pH from 6 to 7.35 and simultaneously measured the  $\text{Ca}^{2+}$  response. The number of responding cells decreased as extracellular pH increased (Figure 2A), and the lower the external pH, the bigger the  $\text{Ca}^{2+}$  release from intracellular stores (Figure 2B). Over the pH range measured, the half-maximal response was seen at pH 7.17 (Figure 2B).

Changes in extracellular pH may affect intracellular pH [6]. We therefore designed experiments to investigate the effect of extracellular acidification on intracellular pH. As shown in Figure 2C, we found a positive correlation between extra- and intracellular acidification. This acidification was still seen after preincubation of cells in the phospholipase C blocker U73122, demonstrating that it was not a consequence of replacement of bound protons by  $\text{Ca}^{2+}$  ions after  $\text{Ca}^{2+}$  release from stores, which could lead to an increase in intracellular free  $\text{H}^+$  concentration and hence a decrease in pH (data not shown). To see whether intracellular acidification contributed to  $\text{Ca}^{2+}$  release from intracellular stores, we applied to the extracellular solution sodium acetate (NaAc), which decreases the intracellular pH without affecting extracellular pH [6].  $\text{IP}_3$  levels were measured in resting cells (pH 7.35) and then after exposure to either extracellular pH 6 or 25 mM NaAc (pH 7.35); the latter procedure led to acidification of intracellular

\*Correspondence: maike.glitsch@dpag.ox.ac.uk

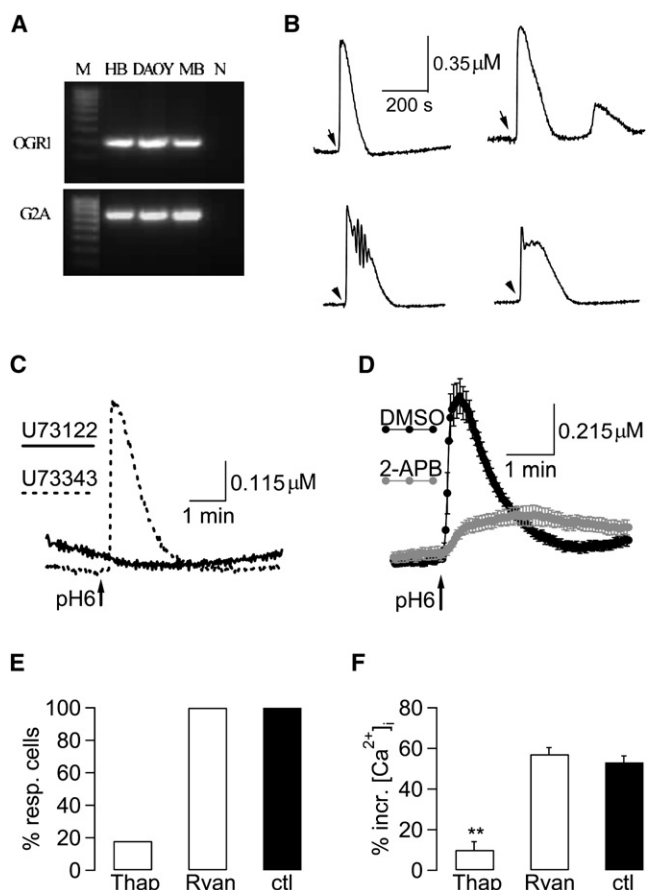


**Figure 1. Extracellular Acidification Triggers  $\text{Ca}^{2+}$  Release from Thapsigargin-Sensitive  $\text{Ca}^{2+}$  Stores via a Phospholipase C-Sensitive Pathway in DAOY Cells**

(A) RT-PCR results from human brain (HB, positive control), DAOY cells (DAOY), and human medulloblastoma tissue (MB) with primers specific for OGR1 (top) and G2A (bottom); N is negative control. Sequencing confirmed the identity of PCR products.

(B) Application of pH 6 in absence of extracellular  $\text{Ca}^{2+}$  (arrow) gave rise to different patterns of intracellular  $\text{Ca}^{2+}$  signals in DAOY cells. Increase in cytosolic  $\text{Ca}^{2+}$  was measured as increase in  $\Delta\text{F}356/\text{F}380$  and was converted to  $\text{Ca}^{2+}$  concentrations. Experiments were done in presence of 0.2 mM ethylene glycol tetraacetic acid (EGTA).

(C) Preincubation of cells with phospholipase C inhibitor U73122 (5  $\mu\text{M}$ ; solid line) for  $83.8 \pm 5$  min or with inactive analog U73343 (5  $\mu\text{M}$ ; dotted line; for  $86.25 \pm 6.6$  min). Drugs were present throughout the experiment, and all experiments were done in absence of external  $\text{Ca}^{2+}$  (0.2 mM EGTA). Arrows indicate switch to pH 6 solution.

(D) Graphs plot increase in intracellular  $\text{Ca}^{2+}$  concentration in presence (gray circles) and absence (black circles) of 30  $\mu\text{M}$  2-APB; experiments in absence of 2-APB were conducted in equivalent concentration of dimethyl sulfoxide (DMSO) (0.1%). Data are represented as mean  $\pm$  standard error of the mean (SEM;  $n = 16$  for DMSO control and 14 for 2-APB); SEM is only given for every second point for clarity.

(E) Bars show percentage of cells responding to application of pH 6 with  $\text{Ca}^{2+}$  release from stores. The black bar indicates control cells, the left white bar thapsigargin-pretreated cells (1–2  $\mu\text{M}$  Thapsigargin for  $69.1 \pm 14.7$  min), and the middle white bar ryanodine-pretreated cells (10  $\mu\text{M}$  ryanodine for  $41.8 \pm 6.6$  min). Experiments were performed in absence of external  $\text{Ca}^{2+}$  (0.2 mM EGTA). Data are represented as mean  $\pm$  SEM.

(F) Bars show percent increase in basal  $\text{Ca}^{2+}$  in responding cells. The black bar indicates control cells ( $n = 19$ ), the left white bar thapsigargin-pretreated cells ( $n = 4$ ), and the middle white bar ryanodine-pretreated cells ( $n = 29$ ). Reduction in  $\text{Ca}^{2+}$  release after thapsigargin pretreatment was significant ( $p < 0.0001$ ; unpaired Student's  $t$  test). Experiments were performed in absence of external  $\text{Ca}^{2+}$  and in presence of 0.2 mM EGTA. Data are represented as mean  $\pm$  SEM.

pH to an extent similar to that seen with extracellular pH 6 (Figure 2D). Despite this, acetate failed to increase  $\text{IP}_3$ ; on the other hand, pH 6 triggered robust  $\text{IP}_3$  production (20 s exposure to either pH 6 or NaAc; Figure 2E), which was transient in nature because we did not observe any significant increase in  $\text{IP}_3$  levels after 50 s exposure to pH 6 ( $p = 0.9084$ ). We also carried out experiments in which we simultaneously recorded intracellular pH and cytoplasmic  $\text{Ca}^{2+}$  release from stores and found that  $\text{Ca}^{2+}$  release preceded intracellular acidification after application of pH 6 solution (Figure 2F), ruling out a decrease in intracellular pH as the cause of  $\text{Ca}^{2+}$  release.

The MAP kinase/ERK pathway is an important regulator of cell proliferation as well as differentiation and apoptosis [7, 8]. Aberrant activation of this pathway is thought to be involved in the formation of tumors [9–11], including medulloblastomas [12]. ERK is activated after a dual phosphorylation by the upstream kinase MEK. Because extracellular acidification is seen as a key factor contributing to tumor growth and invasiveness [1, 2, 13], we examined whether extracellular acidification led to ERK phosphorylation and hence its activation in DAOY cells. Compared with resting cells, extracellular acidification (in 0 mM external  $\text{Ca}^{2+}$ ) led to robust ERK phosphorylation (Figure 3), which was blocked by PD98059, an inhibitor of the upstream ERK activator MEK. ERK phosphorylation was driven by the pH-dependent  $\text{Ca}^{2+}$  release because it was suppressed by pretreating cells with BAPTA-AM (Figure 3). Interestingly, similar levels of ERK phosphorylation after extracellular acidification were observed in the presence of 2 mM external  $\text{Ca}^{2+}$  ( $p = 0.4762$ ). Hence, extracellular pH acidification activates the MEK/ERK pathway in a manner dependent on  $\text{Ca}^{2+}$  release from stores but not  $\text{Ca}^{2+}$  influx.

Changes in membrane potential have been shown to be crucial for regulation and progression of the cell cycle [14–16]. Extracellular acidification can affect the membrane potential by activation of acid-sensing ion channels (ASICs), which are proton-gated ion channels with high  $\text{Na}^+$  permeability [17, 18]. We considered the possibility that the pH-sensing receptor might activate additional types of ion channels because G protein-coupled receptors can regulate channels in a variety of ways, including through G protein subunits [19, 20], DAG (as with canonical transient receptor potential [TRPC] channels [21, 22]),  $\text{Ca}^{2+}$  release from intracellular stores, or store-operated channels [23].

Figure 4A (bottom panel) shows that in DAOY cells, extracellular acidification gave rise to a fast, transient inward current that was followed by a small outward current and a sustained inward current. The latter current was accompanied by a sustained elevation in intracellular  $\text{Ca}^{2+}$  concentration (top panel; see also Figure S2A available online). Table S1 summarizes the effects of extracellular acidification on membrane currents in DAOY cells. Seventeen out of 18 cells displayed the sustained inward current and 12 out of 18 cells the outward current. The fast inward current was also seen in 12 out of 18 cells. This variability might reflect cell-cycle-dependent expression of ion channels [14, 15]. The conductances were dependent entirely on changes in extracellular pH because application of 25 mM NaAc, which triggers intracellular acidification to an extent equivalent to that seen with external pH 6 (Figure 4B), did not give rise to any membrane currents ( $n = 7$ ).

The properties of the initial transient inward current were consistent with activation of ASICs because it developed quickly after changing extracellular pH, rapidly inactivated, and had a positive reversal potential [17, 18]. Because it was very transient (less than 10 s) and not present in all cells, we did not further analyze this conductance.

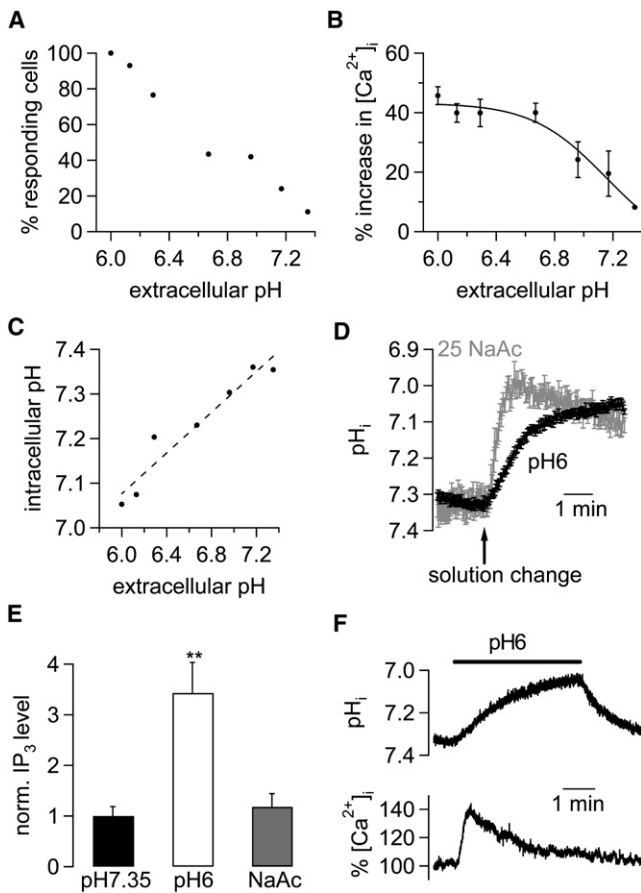


Figure 2. Dependence of Ca<sup>2+</sup> Release from Intracellular Ca<sup>2+</sup> Stores on Extracellular Acidification

(A) Panel plots percentage cells responding to a decrease in extracellular pH with Ca<sup>2+</sup> release from stores for different external pH values. Experiments were performed in the absence of extracellular Ca<sup>2+</sup>.  
 (B) Graph plots increase in cytosolic Ca<sup>2+</sup> levels against extracellular pH value for responding cells (data from two to 54 cells per point, depending on extracellular pH). Experiments were performed in the absence of extracellular Ca<sup>2+</sup>. Data were fitted with a Hill-type equation with the data analysis program Igor Pro (Wavemetric, Oregon), yielding a half-maximal activation of Ca<sup>2+</sup> release at pH 7.17. This was the best fit, but we do not wish to imply a mechanism. Data are represented as mean ± SEM.  
 (C) Plot showing the linear dependence of steady-state intracellular pH versus extracellular pH. Data are from five to 17 cells per data point and are represented as mean ± SEM.  
 (D) Time course of intracellular pH (calibrated from carboxy-SNARF-1 fluorescence) during extracellular acidification (pH 6; black trace; n = 18) or 25 mM sodium acetate (NaAc) solution (at pH 7.35; gray trace; n = 12). The time constant of intracellular pH fall was 20.6 ± 1.35 s for NaAc and 79.4 ± 0.3 s for pH 6 (p < 0.0001, unpaired Student's t test).  
 (E) Panel depicts normalized (norm.) IP<sub>3</sub> level under control (pH 7.35) and test (pH 6, white bar, or 25 mM NaAc, gray bar; 20 s exposure time) conditions; values were normalized to average control levels. All experiments were performed in the absence of extracellular Ca<sup>2+</sup> and Mg<sup>2+</sup>. The increase in IP<sub>3</sub> levels was significant for external pH 6 (p = 0.0085; unpaired Student's t test) for 20 s exposure; there was no significant increase in IP<sub>3</sub> levels after 50 s exposure to pH 6 (data not shown). Data are represented as mean ± SEM.  
 (F) Time course (n = 8) of simultaneously measured intracellular pH (pH<sub>i</sub>, calibrated, top panel) and intracellular Ca<sup>2+</sup> ([Ca<sup>2+</sup>]<sub>i</sub>; expressed as percentage of basal Ca<sup>2+</sup>; bottom panel) during extracellular acidification to pH 6.

Given the composition of our intra- and extracellular recording solutions and holding potential of -50mV, the outward current could be due to either an influx of Cl<sup>-</sup> or an efflux of

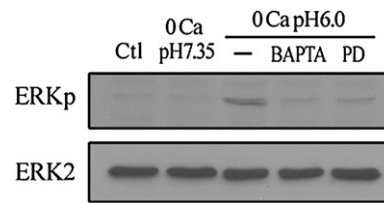


Figure 3. Extracellular Acidification Triggers ERK Phosphorylation

Western blot showing phosphorylation of ERK (ERKp) and total ERK protein (ERK2) under control and test conditions. Medium and pH 7.35 and 0Ca<sup>2+</sup> (with 0.2 mM EGTA) solution did not induce ERK phosphorylation per se (labeled as Ctl and 0Ca pH 7.35, respectively). After exposure to pH 6 and 0Ca<sup>2+</sup> solution (0.2 mM EGTA) for 3 min, there was a clear increase in ERK phosphorylation (0Ca pH 6.0). This increase was not seen when cells were preincubated in 20 μM BAPTA-AM for 50 min (BAPTA; this protocol was shown to prevent acid-induced Ca<sup>2+</sup> release from intracellular Ca<sup>2+</sup> stores; n = 5; data not shown) or when the MEK kinase, which phosphorylates ERK, was blocked by preincubation of cells for 25 min in 50 μM of the MEK kinase blocker PD98059 (PD) prior to application of pH 6 and 0Ca<sup>2+</sup> solution for 3 min. Preincubation of DAOY cells with 50 μM PD98059 for 20–60 min had no effect on the ability of the pH-sensing receptor to trigger Ca<sup>2+</sup> release from intracellular Ca<sup>2+</sup> stores after exposure to pH 6 and 0Ca<sup>2+</sup> solution (n = 9 cells; data not shown).

K<sup>+</sup> ions. We therefore carried out ion-substitution experiments in which we lowered the external Cl<sup>-</sup> concentration from 155.8 to 10.8 mM. A prominent outward current was still observed, suggesting that it was independent of Cl<sup>-</sup> movement and likely reflected a K<sup>+</sup> outward current (Figure S2B). Consistent with this, we measured a smaller outward current with Cs<sup>+</sup> in the patch pipette (145 mM CsCl; data not shown).

The reversal potential of the slow inward current was positive (Figure 4C), on average reversing at +32mV ± 5mV (n = 8). Figure 4A also shows that the fluorescent Ca<sup>2+</sup> signal mirrors the inward current, suggesting that there was significant Ca<sup>2+</sup> influx during the inward current. Consistent with this, we found that the increase in intracellular Ca<sup>2+</sup> concentration after extracellular acidification was significantly larger in the presence of external Ca<sup>2+</sup> than in its absence, suggesting that activation of the pH-sensing receptors triggers Ca<sup>2+</sup> influx (Figure S2C; increase in intracellular Ca<sup>2+</sup> concentration in presence of 2 mM external Ca<sup>2+</sup>: 54.9% ± 2.2%; n = 44; increase in intracellular Ca<sup>2+</sup> concentration in absence of external Ca<sup>2+</sup>: 44.3% ± 2.3%; n = 42; p = 0.0014, unpaired Student's t test).

Because activation of the pH sensor led to Ca<sup>2+</sup> release from intracellular stores, we designed experiments to see whether the acid-induced current was Ca<sup>2+</sup> activated. Dialysis with 20 mM 1,2-Bis(2-aminophenoxy)ethane-N,N,N',N'-tetraacetic acid (BAPTA), which consistently prevented extracellular pH-induced increases in intracellular Ca<sup>2+</sup> concentration, failed to prevent activation of the acid-induced currents (Figure 4D and Figure S2D).

We next tested the effect of phospholipase C blocking, which should prevent the activation of store-operated and TRPC channels. After cells were preincubated with U73122 (which blocked the phospholipase C-induced Ca<sup>2+</sup> release from stores, upper trace), external acidification did not give rise to the sustained inward current, whereas the outward current could still be observed (Figure 4E). Similar results were seen in three more cells, suggesting that blocking of PLC prevented activation of the sustained inward current. Collectively, extracellular acidification activated a Ca<sup>2+</sup>-permeable ion channel in a manner absolutely dependent on phospholipase

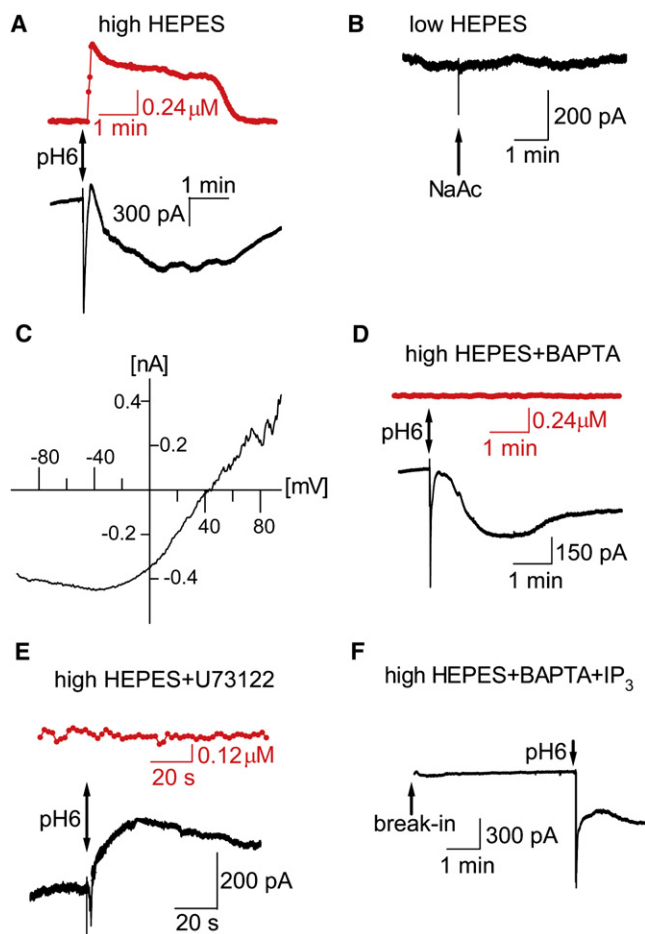


**Figure 4. Extracellular Acidification Activates Three Distinct Ionic Conductances, Including TRPC Channels**

Cells were clamped at  $-50\text{mV}$  (near their resting potential of  $-51.6\text{mV} \pm 6\text{mV}$ ;  $n = 11$ ). External solution always contained  $2\text{mM Ca}^{2+}$ . Changes in intracellular  $\text{Ca}^{2+}$  concentration were monitored with Fura-2. An increase in cytosolic  $\text{Ca}^{2+}$  was seen in 16 out of 18 cells; there was no difference in the extent of the increase in  $\text{Ca}^{2+}$  during patch-clamp experiments compared to imaging experiments only (data not shown).

(A) Experiment performed with standard intracellular solution containing  $30\text{mM HEPES}$  in one representative cell. The upper trace depicts increase in intracellular  $\text{Ca}^{2+}$  concentration, and the bottom trace depicts the change in holding current upon external acidification (arrow). On average, the initial transient inward current peaked after  $4.2 \pm 0.6\text{ s}$  ( $n = 12$ ), the outward current after  $32 \pm 4.7\text{ s}$  ( $n = 12$ ), and the sustained inward current after  $102.9 \pm 12.1\text{ s}$  ( $n = 17$ ).

(B) As in (A), but internal solution with only  $10\text{mM HEPES}$ . Instead of  $\text{pH } 6$ ,  $25\text{mM NaAc}$  was applied.

(C) Graph plots current-voltage relationship ( $-90\text{mV}$  to  $+90\text{mV}$ ) for sustained inward current (ramps given before extracellular acidification were subtracted from ramps obtained during inward current to yield reversal potential of inward current only). Experiments were performed with standard internal solution.

(D) As in (A), but standard internal solution supplemented with  $20\text{mM BAPTA}$  to prevent increases in intracellular  $\text{Ca}^{2+}$  concentration (upper trace; see also Figure S2B).

(E) As in (A), but cell had been preincubated in  $5\text{ }\mu\text{M U73122}$  for  $35\text{ min}$  prior to the experiment.  $\text{Ca}^{2+}$  measurements (top) show that the incubation time was sufficient to block PLC-induced  $\text{Ca}^{2+}$  release from intracellular stores.

(F) Experiment performed with standard intracellular solution containing  $20\text{mM BAPTA}$  and  $30\text{ }\mu\text{M IP}_3$ . Recording was started within  $5\text{ s}$  of breaking into the cell. Store depletion via BAPTA and  $\text{IP}_3$  did not trigger any membrane conductances. Application of  $\text{pH } 6$  and  $2\text{Ca}^{2+}$  solution, however, resulted in transient inward current with prolonged component.

C. We considered that these channels could be either TRPC channels or store-operated ones. To distinguish between these possibilities, we dialysed cells with an internal pipette solution containing  $20\text{mM BAPTA}$  and  $30\text{ }\mu\text{M IP}_3$ , which should deplete intracellular stores, thus triggering store-operated channel opening in the absence of external pH change [24]. Figure 4F shows that up to  $5\text{ min}$  after the cell was broken into, there was no store-operated current (extracellular  $\text{pH } 7.35$ ). Subsequent extracellular acidification, however, gave rise to both the fast and sustained inward currents (Figure 4E;  $n = 6$ ). Hence, store-operated ion channels do not appear to be activated after extracellular acidification. Rather, it seems that the sustained inward current represents a  $\text{Ca}^{2+}$ -permeable TRPC channel [25].

In conclusion, we have shown that extracellular acidification to levels commonly seen in tumors activates intracellular and plasmalemmal  $\text{Ca}^{2+}$  channels, evoking spatially and temporally distinct  $\text{Ca}^{2+}$  signals in a neoplastic neuronal cell line. Cytosolic rises in  $\text{Ca}^{2+}$  can activate distinct processes even in one given cell, depending on where they occur [26]; hence, the activation of two distinct pathways is significant.

Acidification activated  $\text{IP}_3$  receptors and  $\text{Ca}^{2+}$  release from intracellular stores. This recruited the MEK/ERK pathway, providing a mechanistic model whereby extracellular acidification may affect cell growth and proliferation. In addition, acidification also activated a  $\text{Ca}^{2+}$ -permeable nonselective current likely to represent TRPC channels in a manner dependent on phospholipase C activity but independent of  $\text{Ca}^{2+}$  release or store depletion.

In this regard, it is particularly noteworthy that we observed strong expression of G protein coupled pH sensors in primary human tissue from patients with medulloblastoma, a particularly aggressive type of brain tumor. Extracellular acidification is thought to contribute to the progression from benign to malignant growth [1], and those cells capable of tolerating an acidic environment will be able to survive acidification of the microenvironment generally seen in tumor tissue and hence have a proliferative advantage over nontolerant cells, to which this environment is toxic [2]. Our results therefore provide new insight into how acidification can alter neuronal cell function and activate a cellular pathway relevant for tumor pathogenesis with potential therapeutic implications.

#### Supplemental Data

Additional Results and Discussion, Experimental Procedures, two figures, and one table are available at <http://www.current-biology.com/cgi/content/full/18/10/781/DC1/>.

#### Acknowledgments

We are thankful to Prof. A. Parekh for helpful comments on the project and manuscript. We would like to thank Dr. Lynne Cox (Department of Biochemistry, Oxford University, United Kingdom) and Dr. Anne Fowler (DiscoverRx, United Kingdom) for their kind help with  $\text{IP}_3$  measurements. This work was supported by the Royal Society, the John Fell Fund (Oxford University), and the British Heart Foundation.

Received: March 3, 2008

Revised: April 8, 2008

Accepted: April 21, 2008

Published online: May 15, 2008

#### References

1. De Milito, A., and Fais, S. (2005). Tumor acidity, chemoresistance and proton pump inhibitors. *Future Oncol.* 6, 779–786.

2. Gillies, R.J., and Gatenby, R.A. (2007). Hypoxia and adaptive landscapes in the evolution of carcinogenesis. *Cancer Metastasis Rev.* 26, 311–317.
3. Ludwig, M.-G., Vanek, V., Guerini, D., Gasser, J.A., Jones, C.E., Junker, U., Hofstetter, H., Wolf, R.M., and Seuwen, K. (2003). Proton-sensing G-protein coupled receptors. *Nature* 425, 93–98.
4. Seuwen, K., Ludwig, M.-G., and Wolf, R.M. (2006). Receptors for protons or lipid messengers or both? *J. Recept. Signal Transduct. Res.* 26, 599–610.
5. Fais, S., De Milito, A., You, H., and Qin, W. (2007). Targeting vacuolar H<sup>+</sup>-ATPases as a strategy against cancer. *Cancer Res.* 67, 10627–10630.
6. Sun, B., Leem, C.H., and Vaughan-Jones, R.D. (1996). Novel chloride-dependent acid loader in the guinea-pig ventricular myocyte: part of a dual acid-loading mechanism. *J. Physiol.* 495, 65–82.
7. Luttrell, D.K., and Luttrell, L.M. (2003). Signaling in time and space: G protein-coupled receptors and mitogen-activated protein kinases. *Assay Drug Dev. Technol.* 2, 327–338.
8. Rozengurt, E. (2007). Mitogenic signaling pathways induced by G protein-coupled receptors. *J. Cell. Physiol.* 213, 589–602.
9. Dreesen, O., and Brivanlou, A.H. (2007). Signaling pathways in cancer and embryonic stem cells. *Stem Cell Rev.* 3, 7–17.
10. Roberts, P.J., and Der, C.J. (2007). Targeting the Raf-MEK-ERK mitogen-activated protein kinase cascade for the treatment of cancer. *Oncogene* 26, 3291–3310.
11. Junttila, M.R., Li, S.P., and Estermarck, J. (2007). Phosphatase-mediated crosstalk between MAPK signaling pathways in the regulation of cell survival. *FASEB J.*, in press.
12. Włodarski, P., Grajkowska, W., Łojek, M., Rainko, K., and Józwiak, J. (2006). Activation of Akt and Erk pathways in medulloblastoma. *Folia Neuropathol.* 44, 214–220.
13. Laconi, E. (2007). The evolving concept of tumor microenvironments. *Bioessays* 29, 738–744.
14. Kunzelmann, K. (2005). Ion channels and cancer. *J. Membr. Biol.* 205, 159–173.
15. Schreiber, R. (2005). Ca<sup>2+</sup> signaling, intracellular pH and cell volume in cell proliferation. *J. Membr. Biol.* 205, 129–137.
16. Villalonga, N., Ferreres, J.C., Argilés, J.M., Condom, E., and Felipe, A. (2007). Potassium channels are a new target field in anticancer drug design. *Recent Patents Anticancer Drug Discov.* 2, 212–223.
17. Wemmie, J.A., Price, M.P., and Welsh, M.J. (2006). Acid-sensing ion channels: Advances, questions and therapeutic opportunities. *Trends Neurosci.* 29, 578–586.
18. Xiong, Z.-G., Pignataro, G., Li, M., Chang, S.-y., and Simon, R.P. (2008). Acid-sensing ion channels (ASICs) as pharmacological targets for neurodegenerative diseases. *Curr. Opin. Pharmacol.* 8, 25–32.
19. Yi, B.A., Minor, D.L., Jr., Lin, Y.F., Jan, Y.N., and Yan, L.Y. (2001). Controlling potassium channel activities: Interplay between the membranes and intracellular factors. *Proc. Natl. Acad. Sci. USA* 98, 11016–11023.
20. Felix, R. (2005). Molecular regulation of voltage-gated Ca<sup>2+</sup> channels. *J. Recept. Signal Transduct. Res.* 25, 57–71.
21. Trebak, M., Lemonnier, L., Smyth, J.T., Vazquez, G., and Putney, J.W., Jr. (2007). Phospholipase C-coupled receptors and activation of TRPC channels. *Handb. Exp. Pharmacol.* 179, 593–614.
22. Ramsey, S., Delling, M., and Clapham, D.E. (2006). An introduction to TRP channels. *Annu. Rev. Physiol.* 68, 619–647.
23. Parekh, A.B., and Putney, J.W., Jr. (2005). Store-operated calcium channels. *Physiol. Rev.* 85, 757–810.
24. Glitsch, M.D., and Parekh, A.B. (2000). Ca<sup>2+</sup> store dynamics determines the pattern of activation of the store-operated Ca<sup>2+</sup> current I(CRAC) in response to InsP<sub>3</sub> in rat basophilic leukaemia cells. *J. Physiol.* 2, 283–290.
25. Kiselyov, K., Kim, J.Y., Zeng, W., and Muallem, S. (2005). Protein-protein interaction and function TRPC channels. *Eur. J. Phys.* 451, 116–124.
26. Petersen, O.H., and Tepikin, A.V. (2008). Polarized calcium signaling in exocrine gland cells. *Annu. Rev. Physiol.* 70, 273–299.